JACS
JOURNAL OF THE AMERICAN CHEMICAL SOCIETY

Article

pubs.acs.org/JACS

Aggregation of Donor Base Stabilized 2-Thienyllithium in a Single Crystal and in Solution: Distances from X-ray Diffraction and the Nuclear Overhauser Effect

Markus Granitzka,[†] Ann-Christin Pöppler,[†] Eike K. Schwarze,[†] Daniel Stern,[†] Thomas Schulz,[†] Michael John,[†] Regine Herbst-Irmer,[†] Sushil K. Pandey,[‡] and Dietmar Stalke*[,†]

[†]Institut für Anorganische Chemie der Universität Göttingen, Tammannstrasse 4, 37077 Göttingen, Germany

[‡]Department of Chemistry, University of Jammu, Jammu-180 006, India

Supporting Information

ABSTRACT: Various 2-thienyllithium derivatives were investigated in the solid state by X-ray diffraction and in solution by 2D NMR experiments. The determined structures of $[(Et_2O)Li(C_4H_3S)]_4$ (**1**), $[(THF)_2Li(C_4H_3S)]_2$ (**2**), $[(DME)Li(C_4H_3S)]_2$ (**3**), $[(TMEDA)Li(C_4H_3S)]_2$ (**4**), and $[(PMDETA)Li(C_4H_3S)]$ (**5**) (DME = 1,2-dimethoxyethane, TMEDA = *N*,*N*,*N*′,*N*′-tetramethylethylene-1,2-diamine, and PMDETA = *N*,*N*,*N*′,*N*″,*N*″-pentamethyldiethylenetriamine) were solved in nondonating toluene and provide firm ground for diffusion-ordered NMR spectroscopy as well as heteronuclear Overhauser enhancement NMR spectroscopy. The distance relation of nuclear Overhauser effects with a factor of r^{-6} is employed to gain further insight into the aggregation degree of **1**−**5** in solution. Comparison of the slope provided by the linear region of the buildup curves and of the $\sum r^{-6}$ calculated distances from the crystal structures offers a handle to judge the structure retention versus conversion in solution. The structures of **3**−**5** are maintained in toluene solution. The data of **2**, however, indicate a partial dissociation or a rapid exchange between the vertices of a tetrameric core and free THF molecules. Auxiliary exchange spectroscopy investigations showed that the signals of the nitrogen donor base containing compounds **4** and **5** exchange with the signals of nonlithiated thiophene. This is explained by exchange of the deuterium by a hydrogen atom via lithiation of toluene molecules.

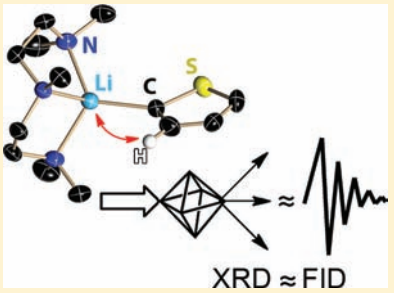

INTRODUCTION

Thiophene, the sulfur-containing five-membered aromatic heterocycle, is one of the most versatile scaffolds in various chemical areas, spanning the wide range from organic synthesis via organometallic chemistry and materials science to life science. In organic syntheses both positions next to the sulfur atom are readily accessible to derivatization,[1] normally starting from a mono- or dihalogenated or -metalated species.[2] Most recently a hetero-s-block-metalated thienyl complex, $[(TMEDA)_2Na,Mg(C_4H_3S)_3]$ (TMEDA = *N*,*N*,*N*′,*N*′-tetramethylethylene-1,2-diamine), was published.[3] Transition-metal thienyl complexes are equally appealing and have been synthesized in past decades in vast variety. More recently they have attracted attention because of their functionality in terms of redox activity, magnetic and fluorescent capability, and optoelectronical performance.[4] Since the award of the chemistry Nobel Prize to Heeger, MacDiarmid, and Shirakawa for the discovery and development of conductive polymers in 2000, polythiophenes (PTs) are one of the most flourishing areas in materials science.[5] They are key candidates for conducting polymers, optoelectronical luminescent layers, sensors, absorbance, and many more applications.[6] Even in anticancer therapy 2,3-disubstituted thiophenes function as signal attenuators in enzyme tracing,[7] and thienyl-substituted titanocenes show a considerably improved cytotoxicity against pig kidney cells (LLC-PK cells).[8]

In all these areas it is also essential to get information about the lithiated species, in the solid state but, even more important, in solution, because structural changes in solution such as solvation and aggregation determine the reactivity and selectivity and hence the product range in organic syntheses and the materials profile of PTs. 2-Monometalation needs to be tuned, i.e., favored or discriminated, against 2,5-dimetalation, because that leaves the thienyl group in either a pendent or bridging position in the product.[9] Even the 3-position can be favored above the 2-position and substituted first while the other remains metalated.[10] Accordingly, besides the well-established issues of solvation and aggregation, valid for any lithium organics, thiophene is a particularly challenging system because of potential mono- and dimetalation in the 2- and/or 3-position.

In his seminal case study on the relationships among solvation, aggregation, and reactivity in organolithium chemistry, Collum stated "X-ray crystallography provides little insight into the thermodynamics of aggregation and solvation."[11] This is right as the crystal structure is commonly

Received: November 4, 2011
Published: December 7, 2011

   dx.doi.org/10.1021/ja210382c | *J. Am. Chem.Soc.* 2012, 134, 1344−1351

believed to represent the least soluble derivative in the pot and not necessarily the most abundant, let alone the most reactive, species. Moreover, the least populated species might represent the eye of the needle in the equilibrium the whole reaction goes through anyway on the course toward the overall product. This was elaborated in several studies on various lithium amides in numerous donating solvents by sophisticated NMR studies.[12] In this paper we tie this in with the present study on 2-thienyllithium coordinated to various donor bases and at different crystallographically assured aggregation states. We synthesized, crystallized, and structurally characterized various 2-thienyllithium aggregates and studied their behavior in solution by 1-D/2-D heteronuclear NMR experiments to start from firm ground and explore their constitution and behavior in solution. The work presented is grounded on the work of Reich et al., who studied the solution structures of 2-thienyllithium with heteronuclear NMR techniques already.[13] The latter paper is based on the case study of the structure–reactivity relationship of phenyllithium in various donor solvents[14] and is mainly focused on side arm donation, not an issue in this work.

RESULTS

Syntheses. We embarked on the synthesis and low-temperature crystallization first. Three different oxygen and two nitrogen donor bases, respectively, should be employed in the study, and we selected Et_2O (diethyl ether), THF (tetrahydrofuran), DME (1,2-dimethoxyethane), TMEDA (*N*,*N*,*N*′,*N*′-tetramethylethylene-1,2-diamine), and PMDETA (*N*,*N*,*N*′,*N*″,*N*″-pentamethyldiethylenetriamine). The lithium derivatives were obtained by a facile reaction between thiophene and *n*-BuLi at 0 °C in a 1:1 stoichiometric ratio in diethyl ether, followed by the addition of the donor bases THF, DME, TMEDA, and PMDETA according to Scheme 1. As

Scheme 1. Preparation of 2-Thienyllithium Derivatives 1–5 via *n*-BuLi at 0 °C in Et_2O Followed by the Addition of the Respective Donor Base

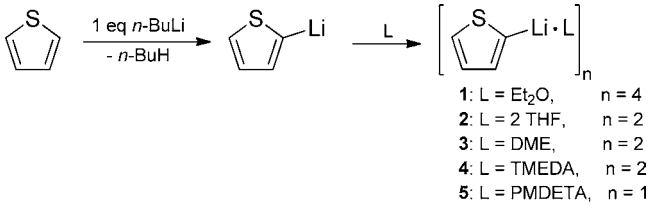

1: L = Et_2O, n = 4
2: L = 2 THF, n = 2
3: L = DME, n = 2
4: L = TMEDA, n = 2
5: L = PMDETA, n = 1

indicated by the pK_a of thiophene (33) compared to that of benzene (44),[15] the heterocycle is readily metalated at the carbon atom next to the ring sulfur but 2,5- and 2,3-dilithiation is also feasible.

Previous Structural Studies. Prior to our work, there were already several structures of 2-thienyllithium derivatives known. First, there are the tetramers with and without donating side arms in the 5-position, $[(THF)_2\{LiC_4H_2(MeO)S\}_4]$[16] and $[(Et_2O)Li\{C_4H_2(Me)S\}]_4$,[17] respectively. Then there are the dimers, also with and without donating side arms in the 5-position, $[(THF)Li\{C_4H_2(MeO)S\}]_2$,[13] $[(TMEDA)Li{\cdot}Li\{(C_4H_2(CH_2NMe_2)S)\}_2]$,[18] $[(THF)Li{\cdot}Li\{C_4H_2(t\text{-}BuN)_2S\text{-}S\}]_2$,[10] $[(TMEDA)Li(C_4H_3S)]_2$,[19] and $[(TMEDA)Li\{C_4H_2(Br)S\}]_2$.[20] In addition, there is the structure of dimeric 2-lithiated benzothiophene $[(TMEDA)Li(C_8H_5S)]_2$.[21] To the best of our knowledge, there is no monomer structurally determined yet. As confirmed by this series of structures again, there is no clear 1:1 relation between donor base and aggregation. Although the infinite solid-state structure of, e.g., $[PhLi]_\infty$[22] in solution is broken down to a $[(Et_2O)LiPh]_4$ tetramer,[23] a $[(TMEDA)LiPh]_2$ dimer[24] on the addition of TMEDA, and a [(PMDETA)LiPh] monomer[25] by adding PMDETA, this deaggregation does not necessarily take place with any other lithium organics, so $[MeLi]_4$ stays tetrameric[26] in diethyl ether solution even upon adding THF, $[(THF)\text{-}LiMe]_4$,[27] or the chelating donor bases TMEDA and DEM (diethoxymethane) to give $[(TMEDA)_2(LiMe)_4]_\infty$[28] and $[(DEM)_{1.5}(LiMe)_4]_\infty$,[29] respectively.

Structure of $[(Et_2O)Li(C_4H_3S)]_4$ (1). The tetramer is the starting point of our investigation and was isolated from the parent reaction mixture upon storing the clear solution at 5 °C. As in all cases, crystals were selected and applied to the diffractometer at cryogenic conditions applying the XTEMP-2 device.[30] **1** crystallizes in the triclinic space group $P\bar{1}$ with one tetramer in the asymmetric unit (Figure 1). The four lithium

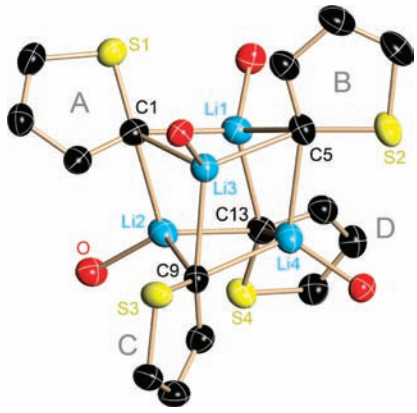

Figure 1. Molecular structure of $[(Et_2O)Li(C_4H_3S)]_4$ (**1**). Anisotropic displacement parameters are depicted at the 50% probability level. Hydrogen atoms and oxygen-bound ethylene groups are omitted for clarity. Note that the thienyl substituents are rotationally disordered relative to the Li_3 plane, indicating no clear preference for additional Li···S interactions. Selected bond distances are displayed in Table 1.

Table 1. Selected Distances (Å) in the Solid-State Structures of 1–5

	av Li···Li	av Li–C_α	Li–O,N[a]	ref
1	2.714(5)	2.282(4)	1.975(7)	this work
2	2.487(3)	2.228(4)	1.979(6)	this work
3	2.504(4)	2.212(14)	2.002(3)	this work
4	2.581	2.187	*2.164*	19
5		2.115(3)	*2.134(2)*	this work

[a]The Li–N bond distances are given in italic type.

atoms form a tetrahedron, a common structural motif for $[LiR]_4$ oligomers.[31] All four almost equilateral Li_3 triangles are μ_3-capped by the C_α atom of the thienyl anion. The average Li–C bond length of 228.2(4) pm is in the range found in the similar tetramer $[(Et_2O)Li\{C_4H_2(Me)S\}]_4$ (average 226.9(2) pm).[17] Recent experimental charge density investigations[32] showed this structural motif also to be present in $[(THF)\text{-}Li_2\{H_2CS(N\text{-}t\text{-}Bu)_2\}]_2$.[33] Up to now the bonding mode and the forces that keep the highly charged Li^+ cations together are not fully understood. It is still controversially discussed as to what extent the Li–C contacts are to be considered as mainly ionic

dx.doi.org/10.1021/ja210382c | J. Am. Chem.Soc. 2012, 134, 1344–1351

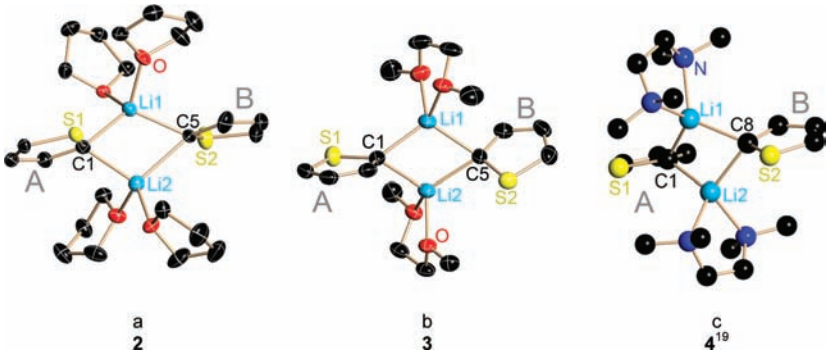

Figure 2. Molecular structures of $[(THF)_2Li(C_4H_3S)]_2$ (**2**) (a), $[(DME)Li(C_4H_3S)]_2$ (**3**) (b), and $[(TMEDA)Li(C_4H_3S)]_2$ (**4**)[19] (c). Anisotropic displacement parameters are depicted at the 50% probability level. Hydrogen atoms are omitted for clarity. Note that the thienyl substituents are rotationally disordered relative to the Li···Li vector, indicating no clear preference for additional Li···S interactions. Selected bond distances are displayed in Table 1.

or showing appreciable covalent contributions.[34] On the basis of the experimental charge density, the interaction of the carbanion with the Li_3 triangle was determined to be a four-center−two-electron (4c−2e) bond. The carbon atom forms a bond path to each of the three lithium atoms. The valence shell charge concentration in the nonbonding region of the carbanion, representing the lone pair, is inclined away from the center of the Li_3 triangle toward the lithium atom at the tip of the isosceles triangle. However, no bond critical points and thus no direct bonding interactions between the lithium atoms were determined.[33] Due to this predominantly ionic interaction, it can rightly be assumed that the aggregation found in the solid state is lowered in solution, preferentially in polar donating solvents. This makes NMR studies in solution particularly important.

Structures of $[(THF)_2Li(C_4H_3S)]_2$ (2), $[(DME)Li(C_4H_3S)]_2$ (3), and $[(TMEDA)Li(C_4H_3S)]_2$ (4). THF is a much better donor to lithium in lithium organics than diethyl ether, because it has a much higher dipole moment (1.75 D for THF vs 1.15 D for Et_2O)[35] and less steric demand. The aggregation of lithium organics normally is lowered by adding one or the other. In addition, it was recently shown that THF can consecutively replace diethyl ether from the coordination of dimeric anthracenyllithium to give $[(THF)_n(Et_2O)_m\{Li(C_{14}H_8)R\}_2]$ dimers, with $n + m = 3$ or 4.[36] Consequently, the addition of THF to a diethyl ether solution of **1** gives crystals of the dimer $[(THF)_2Li(C_4H_3S)]_2$ (**2**) (Figure 2a). Like in many dimers the metalated C_α and lithium atoms form a planar four-membered ring. This ring shows alternating shorter (average 2.174 Å) and longer (average 2.283 Å) Li−C bonds. Those metal atoms which are bonded more tightly are closer to the SC_4H_3 ring plane (Li1 is 1.11 Å from plane A compared to 1.56 Å from plane B) and vice versa (Li2 is 1.32 Å from plane A compared to 0.85 Å from plane B) and accordingly display more σ-bond character to the in-plane lone pair.[36,37]

As anticipated, the two THF donor molecules in the dimer **2** can readily be replaced by the chelating donor base DME. The structure retains the dimeric aggregation with a planar Li_2C_2 four-membered ring to give $[(DME)Li(C_4H_3S)]_2$ (**3**) (Figure 2b). This phenomenon is known from lithium amides and gives rise to the ring stacking and laddering principle.[38] Again, the ring shows alternating shorter (average 2.18 Å) and longer (average 2.24 Å) Li−C bonds. The lithium atom Li1 displays more σ-bond character to thienyl ring A, because it is bonded closer to the related C_α atom and is less displaced from the ring plane (Li1 is 0.97 Å from plane A compared to 1.61 Å from plane B) and vice versa (Li2 is 1.51 Å from plane A compared to 0.52 Å from plane B).[36] The structure of $[(TMEDA)Li(C_4H_3S)]_2$ (**4**) (Figure 2c) was determined earlier.[20] Switching the DME donor base in **3** to TMEDA in **4** has virtually no impact on the structural parameters. The shorter Li−C bonds in the four-membered ring are 2.147 Å long, and the longer ones are 2.228 Å long. The same is true for the σ/π-bonding. The distances of the lithium atoms to the thienyl ring plane are as follows: Li1 is 1.30 Å from plane A compared to 0.92 Å from plane B, and vice versa, Li2 is 1.26 Å from plane A compared to 1.59 Å from plane B.

Structure of $[(PMDETA)Li(C_4H_3S)]$ (5). Providing more than two donor atoms in a single donor base changes the aggregation to monomeric.[31b] In $[(PMDETA)Li(C_4H_3S)]$ (**5**), the lithium atom is coordinated to the single C_α atom in the ring plane like in other lithium aryl monomers (see Figure 3).[25,39] It is only 0.38 Å displaced from the best thienyl plane and hence bonded exclusively to the in-plane lone pair. The Li−C distance of 2.115(3) Å is the shortest in the presented series of thienyllithium structures. Hence, the presented structures mirror a trend already observed in homologous series of other lithium organics: the lower the aggregation, that is the lower the number of Li−C contacts, the shorter the remaining contacts. The mainly ionic metal cation−carbanion attraction is not dispersed to many participants. In the series $[PhLi]_\infty$,[22] $[(Et_2O)LiPh]_4$,[23] $[(TMEDA)LiPh]_2$,[24] and $[(PMDETA)LiPh]$,[25] the distances decrease from 2.32 Å/2.24 Å in the polymer and 2.33 Å in the tetramer to 2.24 Å in

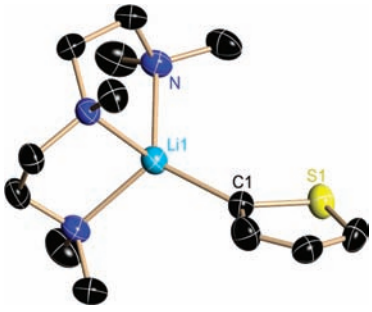

Figure 3. Molecular structure of $[(PMDETA)Li(C_4H_3S)]$ (**5**). Anisotropic displacement parameters are depicted at the 50% probability level. Hydrogen atoms are omitted for clarity. Selected bond distances are displayed in Table 1.

dx.doi.org/10.1021/ja210382c | J. Am. Chem.Soc. 2012, 134, 1344−1351

the dimer and 2.14 Å in the monomer. From the donor-free polymer to the donor base coordinated tetramer, the distances increase because the charge density supply of the donor base leaves the carbanion less attractive to the lithium cation in the tetramer. The trend is not limited to lithium aryls but is also obvious going from $[t\text{-BuLi}]_4$[40] via $[(Et_2O)\text{Li-}t\text{-Bu}]_2$[40] to [{(−)-sparteine}Li-*t*-Bu].[41] Here, the Li−C distances decrease from 2.25 to 2.18 and 2.11 Å.

NMR Investigations of 1−5. Crystals of the aggregates **1**−**4** and the monomer **5** were transferred at inert gas conditions in an argon glovebox to nondonating solvents in NMR tubes and were sealed by septa before being exposed to the experiment. This ensured that we started from known solid state territory into solution that needs to be explored.[42] In general, we first employed routine 1D (^{1}H, ^{13}C, ^{7}Li) experiments and proceeded to the more sophisticated 2D techniques (^{1}H diffusion-ordered NMR spectroscopy (DOSY), ^{1}H,^{7}Li heteronuclear Overhauser enhancement NMR spectroscopy (HOESY)). Due to the low solubility, all NMR spectra of $[(Et_2O)\text{Li}(C_4H_3S)]_4$ (**1**) and $[(\text{TMEDA})\text{Li}(C_4H_3S)]_2$ (**4**) had to be measured with a small excess of the corresponding donor base. As solvent we chose toluene-d_8, which cannot interfere with the coordination sphere of the lithiated thiophenes and the corresponding donor bases. Therefore, one would expect the solvent only disrupts intermolecular contacts present in the crystal while leaving the Li coordination and oligomeric state unchanged.

Figure 4 shows the ^{13}C chemical shifts of the C_α atom which have been used as important indicators for organolithium aggregation before.[13,43] An increase of the ^{13}C chemical shift value from the tetramer **1** to the PMDETA-coordinated monomeric structure **5** is observed, thus confirming the coordination behavior found by single-crystal X-ray diffraction. Furthermore, within the dimeric structures **2**, **3**, and **4**, the ^{13}C chemical shifts show an intriguing correlation with the Li−C_α distances depicted in Table 1. The references above use carbon chemical shifts and ^{13}C−^{6}Li coupling constants to distinguish between different aggregation states by comparing them with each other. Nevertheless, they have not scaled the observed ^{13}C chemical shifts to C_α−Li distances derived from crystal data, which turned out to be fairly significant for our series of compounds. The corresponding ^{1}H and ^{7}Li chemical shifts were much less reproducible and did not follow a clear trend (see the Supporting Information).

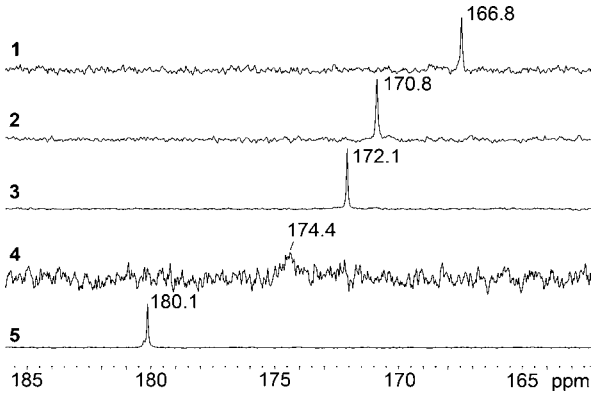

Figure 4. Partial ^{13}C NMR spectra showing the C_α signals of **1**−**5** in toluene-d_8 at room temperature. The poor resolution of the spectrum of **4** is caused by the low solubility in toluene-d_8.

Next, we investigated solutions of **1**−**5** by DOSY.[44] In the past this method has been used extensively to estimate molecular size and aggregation[45] and to detect dynamic behavior.[46] The ^{1}H DOSY spectrum of $[(\text{PMDETA})\text{Li}(C_4H_3S)]$ (**5**) in toluene-d_8 (Figure 5, right) clearly demonstrates that the thienyl group and the donor base form a stable complex as protons from both units display the same diffusion coefficient (1.23×10^{-9} m^2/s). This value is in agreement with the molecular mass (263.37 g/mol) of the monomeric structure. A similar behavior is observed in the ^{1}H DOSY spectra of **3** ($D = 9.3 \times 10^{-10}$ m^2/s) and **4** ($D = 6.3 \times 10^{-10}$ m^2/s). In contrast, in the solution of $[(\text{THF})_2\text{Li}(C_4H_3S)]_2$ (**2**), the observed diffusion coefficient of THF (1.7×10^{-9} m^2/s) varies significantly from that of the metalated thiophene (9.3×10^{-10} m^2/s), but is still substantially lower than that of noncoordinating small molecules such as toluene (2.6×10^{-9} m^2/s) (see Figure 5, left). This indicates that, in solution, THF molecules partially dissociate from the lithiated thiophene structure, possibly leaving Li atoms 3-fold-coordinated. In principle, higher thiophene aggregation would also set free THF molecules; in fact, a dimer−tetramer equilibrium is, for example, known to exist for *n*-BuLi in THF solution.[47] This cannot be finally proven by the low temperature (193 K) reached and would be in disagreement with the chemical shifts of Figure 4.

The ^{1}H DOSY spectra of $[(\text{TMEDA})\text{Li}(C_4H_3S)]_2$ (**4**) and $[(\text{PMDETA})\text{Li}(C_4H_3S)]$ (**5**) show another interesting phenomenon: the apparent diffusion coefficient of the thiophene H-5 signal is slightly larger than that of the protons H-3 and H-4. Closer inspection revealed that this signal slowly decreases with time (6% during one ^{1}H DOSY experiment of 1 h). At the same time an increase of the proton signal assigned to residual

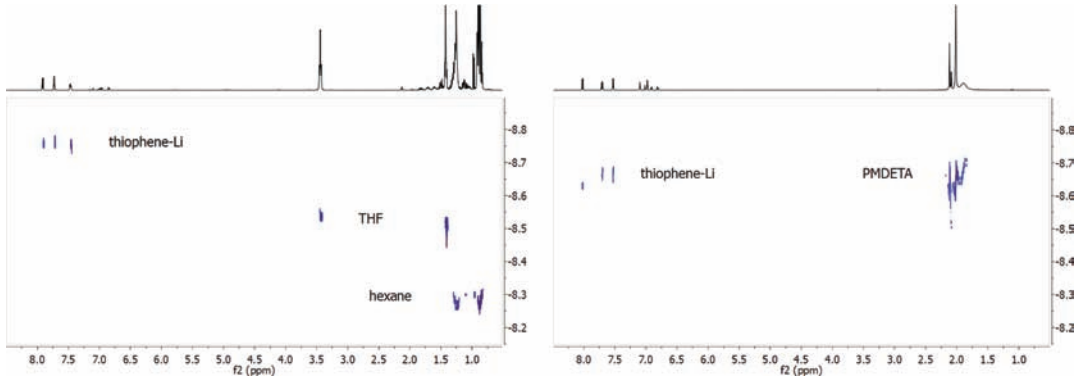

Figure 5. ^{1}H DOSY spectra of $[(\text{THF})_2\text{Li}(C_4H_3S)]_2$ (**2**) (left) and $[(\text{PMDETA})\text{Li}(C_4H_3S)]$ (**5**) (right) in toluene-d_8.

dx.doi.org/10.1021/ja210382c | J. Am. Chem.Soc. 2012, 134, 1344−1351

toluene-d_7 (proton of the methyl group; see the Supporting Information) is observed. This can be explained by exchange of the thiophene H-5 hydrogen atom with deuterium atoms from toluene-d_8 via temporary lithiation of toluene molecules (Scheme 2).

Scheme 2. Exchange Process Triggered by Nitrogen-Containing Donor Bases via Temporary Lithiation of Toluene-d_8

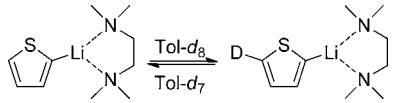

Since the thiophene H-2/H-5 protons are substantially more acidic ($pK_a \approx 33$) compared to the methyl protons of toluene ($pK_a \approx 40$),[48] rametalation of thiophene is fast, and thus, the lithiated toluene intermediate is not detectable by ^{1}H NMR spectroscopy. Interestingly, this H/D exchange was not observed in toluene solutions of **1**–**3**, presumably because oxygen-containing donor bases do not sufficiently increase the thienyl basicity to deprotonate toluene at room temperature.

Finally, compounds **1**–**5** were studied using the ^{1}H,^{7}Li heteronuclear Overhauser effect (HOE). Since the crystal structures contain several short proton–lithium distances (up to 4 Å), cross-peaks should appear in ^{1}H,^{7}Li HOESY spectra that either prove or disprove the solid-state structure in solution. Figure 6 depicts the ^{1}H,^{7}Li HOESY NMR spectrum of

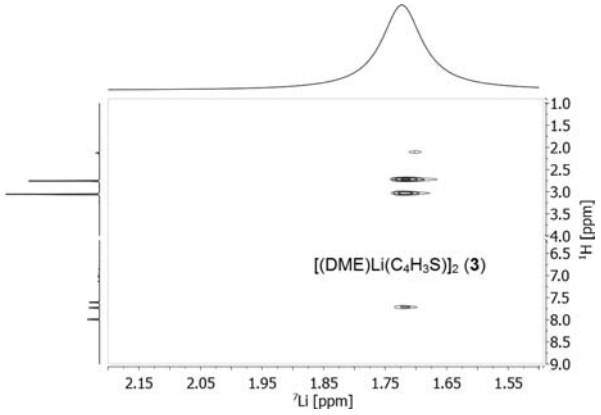

Figure 6. ^{1}H,^{7}Li HOESY spectrum (mixing time 0.5 s) of $[(DME)Li(C_4H_3S)]_2$ (**3**) exhibiting cross-peaks between lithium and the related thienyl moiety and the corresponding donor base.

3 in toluene-d_8 as an example (spectra of the other compounds are shown in the Supporting Information). In addition to the cross-peaks to the neighboring proton (H-3) of the thiophene moiety, each spectrum displays cross-peaks to the corresponding donor bases (Et_2O, THF, DME, TMEDA, and PMDETA). By varying the mixing time from 0.01 to 1.0 s, we recorded buildup curves (Figure 7 and Supporting Information). All curves feature an initial linear increase of the cross-peak intensity and a maximum after approximately 0.5 s followed by a decay of the intensity at higher mixing times due to relaxation.[49]

Assuming a linear relationship between the slope of the initial buildup and the inverse sixth power of the proton–lithium distance,[50] comparison of that slope with the $\sum r(H\cdots Li)^{-6}$ term calculated from the crystal structures offers a handle to

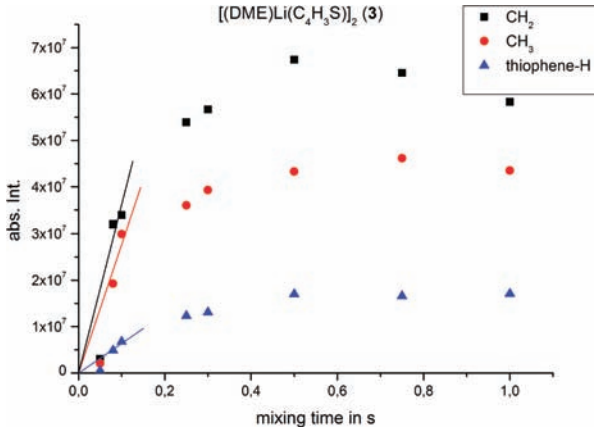

Figure 7. Buildup curves of the ^{1}H,^{7}Li HOESY spectrum of $[(DME)Li(C_4H_3S)]_2$ (**3**) in toluene-d_8. Mixing times were varied between 0.01 and 1.0 s. Cross-peaks could be observed for the neighboring thiophene proton and the CH_2/CH_3 groups of DME.

judge whether the structures are retained in solution. Due to the low solubility of **1**, cross-peaks could be observed, but they were not sufficiently strong for really short mixing times, preventing them from being included in this comparison.

Figure 8 clearly demonstrates good agreement between distances derived from ^{1}H,^{7}Li HOESY experiments and the

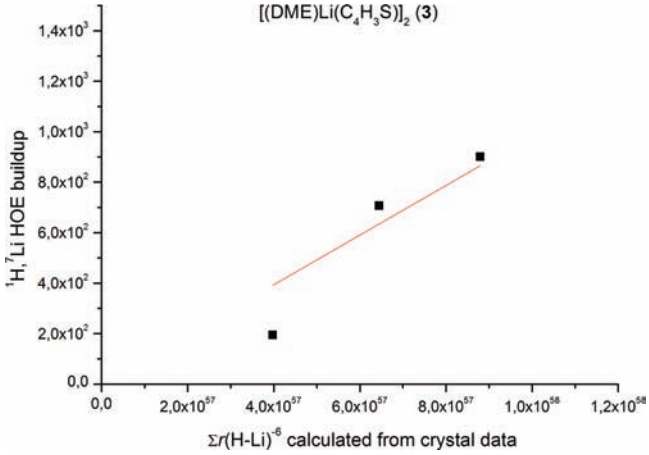

Figure 8. Comparison of the ^{1}H,^{7}Li HOE buildup with the calculated $\sum r(H\cdots Li)^{-6}$ terms from crystal data of **3**. Disorders in the crystal have been taken into account for these calculations.

crystal structure. Slight deviations may originate from intramolecular motions that affect the HOE in solution. Since similar plots were obtained for compounds **4** and **5**, we conclude that the structures of **3**–**5** are retained upon dissolving in toluene. The different behavior of **2** already indicated by ^{1}H DOSY NMR is mirrored by the HOESY data: Compared to what is expected from the crystal data, the cross-peaks belonging to the THF protons are much too weak. Again, this would be explained by a partial dissociation of THF molecules from a dimeric core or, alternatively, THF molecules rapidly exchanging between the vertices of a tetrameric core and free solution. With regard to the latter explanation, it should be noted that $\sum r(H\cdots Li)^{-6}$ for a conceivable tetrameric structure $[(THF)Li(C_4H_3S)]_4$ is in very good congruency with the measured HOESY data (see the Supporting Information).

dx.doi.org/10.1021/ja210382c | J. Am. Chem.Soc. 2012, 134, 1344–1351

Table 2. Selected Crystallographic Data for 1−3 and 5

	1	2	3	5
cryst syst	triclinic	triclinic	triclinic	monoclinic
space group	$P\bar{1}$	$P\bar{1}$	$P\bar{1}$	$P2_1/n$
CCDC no.	833247	833248	833249	833250
temp, K	99(2)	100(2)	100(2)	100(2)
cryst size, mm	0.20 × 0.12 × 0.10	0.30 × 0.20 × 0.20	0.20 × 0.12 × 0.10	0.1 × 0.1 × 0.05
empirical formula	$C_{32}H_{52}Li_4O_4S_4$	$C_{24}H_{38}Li_2O_4S_2$	$C_{16}H_{26}Li_2O_4S_2$	$C_{13}H_{26}LiN_3S$
Z	2	2	2	4
formula mass	656.74	468.54	360.37	263.37
unit cell length a, Å	10.086(2)	9.303(2)	8.625(2)	8.466(2)
unit cell length b, Å	11.779(2)	9.531(3)	10.471(2)	15.573(3)
unit cell length, c, Å	17.970(3)	14.945(2)	12.749(2)	12.226(2)
unit cell angle α, deg	85.97(2)	97.29(2)	76.66(2)	90
unit cell angle β, deg	73.83(2)	97.15(2)	81.73(2)	93.36(2)
unit cell angle γ, deg	66.45(2)	98.03(2)	67.47(2)	90
vol, Å^3	1877.6(6)	1287.8(4)	1032.9(3)	1609.1(6)
ρ_{calcd}, g/cm^3	1.162	1.208	1.159	1.087
$F(000)$	704	504	384	576
θ range, deg	1.18−26.39	2.41−26.39	2.15−26.73	2.12−25.71
no. of collected reflns	44903	25595	20286	17890
no. of independent reflns	7676	5251	4378	3055
R_{int}	0.0550	0.0230	0.0421	0.0326
no. of data/restraints/params	7676/1074/594	5251/1498/535	4378/322/313	3055/138/214
R1, wR2 $[I \geq 2\sigma(I)]^{a,b}$	0.0429, 0.1055	0.0362, 0.0916	0.0421, 0.1108	0.0332, 0.0814
R1, wR2 (all data)	0.0620, 0.1163	0.0410, 0.0943	0.0538, 0.1184	0.0467, 0.0863
goodness-of-fit	1.066	1.048	1.045	1.059
$g_1/g_2{}^c$	0.0521/0.5626	0.0435/0.5012	0.0638/0.2645	0.0438/0.2014
largest diff peak/hole, e Å^{-3}	0.320/−0.455	0.391/−0.223	0.504/−0.173	0.153/−0.150

^{a}R1 = $\sum||F_o| - |F_c||/\sum|F_o|$. ^{b}wR2 = $[\sum w(F_o^2 - F_c^2)^2/\sum w(F_o^2)^2]^{0.5}$. $^c w = [\sigma^2(F_o^2) + (g_1P)^2 + g_2P]^{-1}$, $P = 1/3[\max(F_o^2,0)+2F_c^2]$.

CONCLUSION

In the solid state 2-thienyllithium forms the tetramer $[(Et_2O)Li(C_4H_3S)]_4$ (**1**) when exposed to the donor base diethyl ether, the dimers $[(THF)_2Li(C_4H_3S)]_2$ (**2**), $[(DME)Li(C_4H_3S)]_2$ (**3**), and $[(TMEDA)Li(C_4H_3S)]_2$ (**4**) when subjected to tetrahydrofuran, dimethoxyethane, and *N*,*N*,*N*′,*N*′-tetramethylethylene-1,2-diamine, and the monomer $[(PMDETA)Li(C_4H_3S)]$ (**5**) when exposed to the tridentate *N*,*N*,*N*′,*N*″,*N*″-pentamethyldiethylenetriamine. The distance relation of Li···H nuclear Overhauser effects is employed to gain insight into the aggregation degree of **1**−**5** in nondonating solution. Comparison of the slope provided by the linear region of the buildup curves and of the $\sum r^{-6}$ calculated distances from the crystal structures confirmed that the structures of **3**−**5** are maintained in toluene solution. Exchange spectroscopy investigations showed that the signals of nitrogen donor base containing compounds **4** and **5** exchange with the signals of nonlithiated thiophene. This is explained by exchange of the deuterium by a hydrogen atom via lithiation of toluene molecules followed by protonation. In an additional experiment, it would be interesting to investigate whether the same structure is retained in different solvents by solvent swapping. If the two structures differ only in the solvation shell, swapping one solvent for another would only cause a migration of the resonance without a change in resonance count.[51]

EXPERIMENTAL SECTION

General Procedure. To a solution of thiophene (2.0 mL, 27.6 mmol) in 20 mL of diethyl ether was added a solution of 1 equiv of *n*-BuLi (1.51 M in *n*-hexane) over 30 min at 0 °C. An excess of donor base (2.5 equiv) was added followed by constant stirring for another 30 min. The solution was then cooled to −78 °C. The crystals thus formed were filtered, washed twice with precooled *n*-hexane (−78 °C), and finally dried in vacuo. This general method was applied for the synthesis of all presented compounds (**1**−**5**).

NMR spectra were recorded on a Bruker Avance III 400 MHz spectrometer (Bruker Biospin, Rheinstetten, Germany) with a broadband observe probe, *z*-gradient, and temperature unit. The spectra were recorded at various temperatures in toluene-d_8. All spectra were processed with Topspin 2.1 (Bruker Biospin) and further plotted with MestreNova, version 7.0 (Mestrelab Research, Santiago de Compostela, Spain).

[2-Thienyllithium·Et$_2$O]$_4$ (1). Colorless crystals were obtained in a yield of 2.4 g (3.6 mmol, 52%): $C_{32}H_{52}Li_4O_4S_4$ (656.74 g/mol); ^{1}H NMR (C_7D_8) δ 7.80 (d, $^3J_{HH}$ = 4.3 Hz, 1 H, H_5), 7.63 (d, $^3J_{HH}$ = 2.7 Hz, 1 H, H_3), 7.33 (dd, $^3J_{HH}$ = 4.3 Hz, $^3J_{HH}$ = 2.8 Hz, 1H, H_4), 3.19 (q, $^3J_{HH}$ = 7.0 Hz 6 H, CH_3), 0.96 (t, $^3J_{HH}$ = 7.0 Hz 4 H, CH_2); ^{13}C{^{1}H} NMR (C_7D_8) δ 166.9 (C_2), 137.5 (C_5), 133.1 (C_3), 128.1 (C_4), 65.7 (CH_3), 15.1 (CH_2); ^{7}Li{^{1}H} NMR δ 2.1 (s).

[2-Thienyllithium·2THF]$_2$ (2). Colorless crystals were obtained in a yield of 1.2 g (2.6 mmol, 18.5%): $C_{24}H_{38}Li_2O_4S_2$ (468.54 g/mol); ^{1}H NMR (C_7D_8) δ 7.88 (d, $^3J_{HH}$ = 4.3 Hz, 1 H, H_5), 7.70 (dd, $^3J_{HH}$ = 2.7 Hz, $^4J_{HH}$ = 2.4 Hz, 1 H, H_3), 7.430 (dd, $^3J_{HH}$ = 4.28 Hz, $^3J_{HH}$ = 2.76 Hz, 1H, H_4), 3.41 (m, 8 H, OCH_2), 1.39 (m, 8 H, CH_2); ^{13}C{^{1}H} NMR (C_7D_8) δ 170.9 (C_2), 137.2 (C_5), 131.6 (C_3), 127.7 (C_4), 65.7 (OCH_2), 25.7 (CH_2); ^{1}Li{^{1}H} NMR δ 1.9 (s).

[2-Thienyllithium·DME]$_2$ (3). Colorless crystals were obtained in a yield of 3.6 g (10.0 mmol, 79%): $C_{16}H_{26}Li_2O_4S_2$ (360.39 g/mol); ^{1}H NMR (C_7D_8) δ 7.95 (dd, $^3J_{HH}$ = 4.3 Hz, $^4J_{HH}$ = 0.4 Hz, 1 H, H_5), 7.69 (dd, $^3J_{HH}$ = 2.8 Hz, $^4J_{HH}$ = 0.4 Hz, 1 H, H_3), 7.57 (dd, $^3J_{HH}$ = 4.4 Hz, $^3J_{HH}$ = 2.8 Hz, 1 H, H_4), 3.02 (s, 6 H, CH_3), 2.72 (s, 4 H, CH_2); ^{13}C{^{1}H} NMR (C_7D_8) δ 172.1 (C_2), 136.5 (C_5), 130.7 (C_3), 127.5 (C_4), 70.1 (CH_3), 58.8 (CH_2); ^{7}Li{^{1}H} NMR δ 1.7 (s).

[2-Thienyllithium·TMEDA]$_2$ (4). Yellow crystals were obtained in a yield of 2.8 g (6.8 mmol, 49%): $C_{20}H_{38}Li_2N_4S_2$ (412.55 g/mol); ^{1}H

dx.doi.org/10.1021/ja210382c | J. Am. Chem.Soc. 2012, 134, 1344−1351

NMR (C_7D_8) δ 7.92 (d, $^3J_{HH}$ = 5.0 Hz, 1 H, H_5), 7.66 (br s, 1 H, H_3), 7.50 (d, $^3J_{HH}$ = 4.8 Hz, 1 H, H_4), 2.28 (s, 12 H, CH_3), 2.09 (s, 4 H, CH_2); $^{13}C\{^1H\}$ NMR (C_7D_8) δ 174.4 (C_2), 137.2 (C_5), 130.8 (C_3), 127.4 (C_4), 58.4 (CH_2), 46.0 (CH_3); $^7Li\{^1H\}$ NMR δ 2.0 (s).

[2-Thienyllithium·PMDETA] (5). Light red crystals were obtained in a yield of 3.4 g (12.9 mmol, 47%): $C_{13}H_{26}LiN_3S$ (263.3 g/mol); ^1H NMR (C_7D_8) δ 7.95 (dd, $^3J_{HH}$ = 4.2 Hz, $^4J_{HH}$ = 0.4 Hz, 1 H, H_5), 7.64 (dd, $^3J_{HH}$ = 4.2 Hz, $^3J_{HH}$ = 2.7 Hz, 1 H, H_4), 7.49 (dd, $^3J_{HH}$ = 2.7 Hz, $^4J_{HH}$ = 0.4 Hz, 1 H, H_3), 2.11 (s, 3 H, NCH_3), 2.01 (s, 12 H, $N(CH_3)_2$), 1.86 (br, 8 H, CH_2); $^{13}C\{^1H\}$ NMR (C_7D_8) δ 180.1 (C_2), 137.5 (C_5), 133.3 (C_3) 126.8 (C_4), 57.3 (Me_2NCH_2), 53.9 (CH_2NMe), 45.9 ($N(CH_3)_2$), 44.6 (NCH_3); $^7Li\{^1H\}$ NMR δ 2.1 (s).

Single-Crystal Structural Analysis. Single crystals were selected from a Schlenk flask under an argon atmosphere and covered with perfluorated polyether oil on a microscope slide, which was cooled with a nitrogen gas flow using the X-TEMP2.[30] An appropriate crystal was selected using a polarized microscope, mounted on the tip of a MiTeGen MicroMount or glass fiber, fixed to a goniometer head, and shock cooled by the crystal cooling device.

The data for **1**−**3** and **5** were collected from shock-cooled crystals at 100(2) K.[30] The data for **1** were collected on an Incoatec Mo microsource[52] with mirror optics and an APEX II detector with a D8 goniometer. The data for **2**, **3**, and **5** were measured on a Bruker TXS-Mo rotating anode with mirror optics and an APEX II detector with a D8 goniometer. Both diffractometers were equipped with a low-temperature device and used Mo Kα radiation, λ = 71.073 pm. The data for **1**−**3** and **5** were integrated with SAINT,[53] and an empirical absorption correction (SADABS)[54] was applied. The structures were solved by direct methods (SHELXS-97)[55a] and refined by full-matrix least-squares methods against F^2 (SHELXL-97)[55b,c] within the SHELXLE GUI.[55d] All non-hydrogen atoms were refined with anisotropic displacement parameters. The hydrogen atoms were refined isotropically on calculated positions using a riding model with their U_{iso} values constrained to equal 1.5 times the U_{eq} of their pivot atoms for terminal sp^3 carbon atoms and 1.2 times for all other carbon atoms. Disordered moieties were refined using bond length restraints and anisotropic displacement parameter restraints.

Crystallographic data (excluding structure factors) for the structures reported in this paper have been deposited with the Cambridge Crystallographic Data Centre. The CCDC numbers, crystal data, and experimental details for the X-ray measurements are listed in Table 2. Copies of the data can be obtained free of charge from the Cambridge Crystallographic Data Centre via www.ccdc.cam.ac.uk/data_request/cif or from the corresponding author.

Crystallographic data for **4** are taken from the literature.[19]

■ ASSOCIATED CONTENT

Supporting Information

Further experimental details and physical and spectroscopic data for **1**−**5** and CIF data. This material is available free of charge via the Internet at http://pubs.acs.org.

■ AUTHOR INFORMATION

Corresponding Author

dstalke@chemie.uni-goettingen.de

■ ACKNOWLEDGMENTS

We thank the Deutsche Forschungsgemeinschaft (DFG) Priority Programme 1178 and the Danish National Research Foundation (DNRF) funded Center for Materials Crystallography (CMC) for support and the Land Niedersachsen for providing a fellowship in the Catalysis for Sustainable Synthesis (CaSuS) Ph.D. program.

■ REFERENCES

(1) Biehl, E. R. *Prog. Heterocycl. Chem.* **2011**, *22*, 109−141.
(2) Chinchilla, R.; Nájera, C.; Yus, M. *ARKIVOC* **2007**, *10*, 152−231.
(3) Blair, V. L.; Kennedy, A. R.; Mulvey, R. E.; O'Hara, C. T. *Chem.—Eur. J.* **2010**, *16*, 8600−8604.
(4) Belo, D.; Almeida, M. *Coord. Chem. Rev.* **2010**, *254*, 1479−1492.
(5) *Handbook of Thiophene-Based Materials: Applications in Organic Electronics and Photonics* [Online]; John Wiley & Sons: Chichester, U.K., 2009. http://www.amazon.com/Handbook-Thiophene-Based-Materials-Applications-Electronics/dp/0470057327, accessed 7/27/11.
(6) For a review see, e.g.: Liu, Y.; Liu, Y.; Zhan, X. *Macromol. Chem. Phys.* **2011**, *212*, 428−443.
(7) Petti, F.; Thelemann, A.; Kahler, J.; McCormack, S.; Castaldo, L.; Hunt, T.; Nuwaysir, L.; Zeiske, L.; Haack, H.; Sullivan, L.; Garton, A.; Haley, J. D. *Mol. Cancer Ther.* **2005**, *4*, 1186−1197.
(8) Sweeney, N. J.; Gallagher, W. M.; Müller-Bunz, H.; Pampillón, C.; Strohfeldt, K.; Tacke, M. *J. Inorg. Biochem.* **2006**, *100*, 1479−1486.
(9) Selinka, C.; Stalke, D. *Eur. J. Inorg. Chem.* **2003**, 3376−3382.
(10) Selinka, C.; Stalke, D. *Z. Naturforsch.* **2003**, *58b*, 291−298.
(11) Collum, D. B. *Acc. Chem. Res.* **1992**, *25*, 448−454.
(12) (a) DePue, J. S.; Collum, D. B. *J. Am. Chem. Soc.* **1988**, *110*, 5518−5524. (b) DePue, J. S.; Collum, D. B. *J. Am. Chem. Soc.* **1988**, *110*, 5524−5533. (c) Galiano-Roth, A. S.; Collum, D. B. *J. Am. Chem. Soc.* **1989**, *111*, 6772−6778. (d) Remenar, J. F.; Collum, D. B. *J. Am. Chem. Soc.* **1998**, *120*, 4081−4086.
(13) (a) Jantzi, K. L.; Puckett, C. L.; Guzei, I. A.; Reich, H. J. *J. Org. Chem.* **2005**, *70*, 7520−7529. (b) Reich, H. J.; Whipple, W. L. *Can. J. Chem.* **2005**, *83*, 1577−1587.
(14) Reich, H. J.; Green, D. P.; Medina, M. A.; Goldenberg, W. S.; Gudmundsson, B. O.; Dykstra, R. R.; Phillips, N. H. *J. Am. Chem. Soc.* **1998**, *120*, 7201−7210.
(15) Shen, K.; Fu, Y.; Li, J.-N.; Liu, L.; Guo, Q.-X. *Tetrahedron* **2007**, *63*, 1568−1576.
(16) Spek, A. L.; Veldman, N. Private communication to the Cambridge Crystallographic Data Centre, 1999; RefCode HIGPOC.
(17) Powell, D. R.; Whipple, W. L.; Reich, H. J. *Acta Crystallogr., Sect. C* **1996**, *52*, 1346−1348.
(18) Spek, A. L., Lakin, M. T.; den Besten, R. Private communication to the Cambridge Crystallographic Data Centre, 1999; RefCode LEDSES.
(19) Spek, A. L., Smeets, W. J. J. Private communication to the Cambridge Crystallographic Data Centre, 1999; RefCode JUJXER.
(20) Spek, A. L. Private communication to the Cambridge Crystallographic Data Centre, 1999; RefCode HIGXUQ.
(21) Harder, S.; Boersma, J.; Brandsma, L.; Kanters, J. A.; Bauer, W.; Pi, R.; Schleyer, P. v. R.; Schöllhorn, H.; Thewalt, U. *Organometallics* **1989**, *8*, 1688−1696.
(22) Dinnebier, R. E.; Behrens, U.; Olbrich, F. *J. Am. Chem. Soc.* **1998**, *120*, 1430−1433.
(23) Hope, H.; Power, P. P. *J. Am. Chem. Soc.* **1983**, *105*, 5320−5324.
(24) Thoennes, D.; Weiss, E. *Chem. Ber.* **1978**, *111*, 3157−3161.
(25) Schümann, U.; Kopf, J.; Weiss, E. *Angew. Chem.* **1985**, *97*, 222−223; *Angew. Chem., Int. Ed. Engl.* **1985**, *24*, 215−216.
(26) Weiss, E.; Lambertsen, T.; Schubert, B.; Cockcroft, J. K.; Wiedenmann, A. *Chem. Ber.* **1990**, *123*, 79−81.
(27) Ogle, C. A.; Huckabee, B. K.; Johnson, H. C. IV; Sims, P. F.; Winslow, S. D.; Pinkerton, A. A. *Organometallics* **1993**, *12*, 1960−1963.
(28) Köster, H.; Thoennes, D.; Weiss, E. *J. Organomet. Chem.* **1978**, *160*, 1−5.
(29) Walfort, B.; Lameyer, L.; Weiss, W.; Herbst-Irmer, R.; Bertermann, R.; Rocha, J.; Stalke, D. *Chem.—Eur. J.* **2001**, *7*, 1417−1423.
(30) (a) Kottke, T.; Stalke, D. *J. Appl. Crystallogr.* **1993**, *26*, 615−619. (b) Kottke, T.; Lagow, R. J.; Stalke, D. *J. Appl. Crystallogr.* **1996**, *29*, 465−468. (c) Stalke, D. *Chem. Soc. Rev.* **1998**, *27*, 171−178.
(31) (a) Gessner, V. H.; Däschlein, C.; Strohmann, C. *Chem.—Eur. J.* **2009**, *15*, 3320−3334. (b) Stey, T.; Stalke, D. Lead structures in lithium organic chemistry. In *The Chemistry of Organolithium Compounds*; Rappoport, Z., Marek, I., Eds.; John Wiley & Sons: Chichester, U.K., 2004; pp 47−120; (c) Stalke, D. *Angew. Chem.* **1994**,

106, 2256−2259; *Angew. Chem., Int. Ed. Engl.* **1994**, *33*, 2168−2171. (d) Weiss, E. *Angew. Chem.* **1993**, *105*, 1565−1587;(e) *Angew. Chem., Int. Ed. Engl.* **1993**, *32*, 1501−1523. (f) Setzer, W. N.; Schleyer, P. v. R. *Adv. Organomet. Chem.* **1985**, *24*, 353−451. (g) Schleyer, P. v. R. *Pure Appl. Chem.* **1983**, *55*, 355−362.

(32) Stalke, D. *Chem.—Eur. J.* **2011**, *17*, 9264−9278.

(33) Deuerlein, S.; Leusser, D.; Flierler, U.; Ott, H.; Stalke, D. *Organometallics* **2008**, *27*, 2306−2315.

(34) (a) Bickelhaupt, F. M.; Solà, M.; Guerra, C. F. *J. Chem. Theory Comput.* **2006**, *2*, 965−980. (b) Matito, E.; Poater, J.; Bickelhaupt, F. M.; Solà, M. *J. Phys. Chem. B* **2006**, *110*, 7189−7198.

(35) *CRC Handbook of Chemistry and Physics*, 87th ed.; Lide, D. R., Ed.; Chemical Rubber Publishing Co.: Boca Raton, FL, 2006.

(36) Stern, D.; Finkelmeier, N.; Meindl, K.; Henn, J.; Stalke, D. *Angew. Chem.* **2010**, *122*, 7021−7024; *Angew. Chem., Int. Ed.* **2010**, *49*, 6869−6872.

(37) Stalke, D.; Whitmire, K. H. *Chem. Commun.* **1990**, 833−834.

(38) (a) Gregory, K.; Schleyer, P. v. R.; Snaith, R. *Adv. Inorg. Chem.* **1991**, *37*, 47−142. (b) Mulvey, R. E. *Chem. Soc. Rev.* **1991**, *20*, 167−209.

(39) Schiemenz, B.; Power, P. P. *Angew. Chem.* **1996**, *108*, 2288−2290; *Angew. Chem., Int. Ed. Engl.* **1996**, *35*, 2150−2151.

(40) Kottke, T.; Stalke, D. *Angew. Chem.* **1993**, *105*, 619−621; *Angew. Chem., Int. Ed. Engl.* **1993**, *32*, 580−582.

(41) Strohmann, C.; Seibel, T.; Strohfeldt, K. *Angew. Chem.* **2003**, *115*, 4669−4671; *Angew. Chem., Int. Ed.* **2003**, *42*, 4531−4533.

(42) (a) Edelmann, F. T.; Knösel, F.; Pauer, F.; Stalke, D.; Bauer, W. *J. Organomet. Chem.* **1992**, *438*, 1−10. (b) Hoffmann, D; Bauer, W.; Schleyer, P. v. R.; Pieper, U.; Stalke, D. *Organometallics* **1993**, *12*, 1193−1200.

(43) For examples see (a) Kühnen, M.; Günther, H.; Amoureux, J.-P.; Fernandéz, C. *Magn. Reson. Chem.* **2002**, *40*, 24−30. (b) Seebach, D.; Hässig, R.; Gabriel, J. *Helv. Chim. Acta* **1983**, *66*, 308−337. (c) Fraenkel, G.; Chow, A.; Winchester, W. R. *J. Am. Chem. Soc.* **1990**, *112*, 6190−6198.

(44) Li, W.; Kagan, G.; Hopson, R.; Williard, P. G. *ARKIVOC* **2011**, *5*, 180−187.

(45) (a) Valentini, M.; Pregosin, P. S.; Rüegger, H. *Organometallics* **2000**, *19*, 2551−2555. (b) Keresztes, I.; Williard, P. G. *J. Am. Chem. Soc.* **2000**, *122*, 10228−10229. (c) Li, D.; Sun, C.; Liu, J.; Hopson, R.; Li, W.; Williard, P. G. *J. Org. Chem.* **2008**, *73*, 2373−2381.

(46) Hassinen, A.; Moreels, I.; Donegá, C. d. M.; Martins, J. C.; Hens, Z. *J. Phys. Chem. Lett.* **2010**, *1*, 2577−2581.

(47) Heinzer, J.; Oth, J. F. M.; Seebach, D. *Helv. Chim. Acta* **1985**, *68*, 1848−1862.

(48) *March's Advanced Organic Chemistry*, 6th ed.; Smith, M. B., March, J., Eds.; Wiley-Interscience: Hoboken, NJ, 2007.

(49) Neuhaus, D.; Williamson, M. P. *The Nuclear Overhauser Effect in Structural and Conformational Analysis*; VCH: New York, 1989.

(50) Gronenborn, A. M.; Clore, G. M. *Prog. Nucl. Magn. Reson. Spectrosc.* **1985**, *17*, 1−36.

(51) De Vries, T. S.; Goswami, A.; Liou, L. R.; Gruver, J. M.; Jayne, E.; Collum, D. B. *J. Am. Chem. Soc.* **2009**, *131*, 13142−13154.

(52) Schulz, T.; Meindl, K.; Leusser, D.; Stern, D.; Graf, J.; Michaelsen, C.; Ruf, M.; Sheldrick, G. M.; Stalke, D. *J. Appl. Crystallogr.* **2009**, *42*, 885−891.

(53) *SAINT*, version 7.68A; *Bruker APEX*, version 2011.9; Bruker AXS: Madison, WI, 2008.

(54) Sheldrick, G. M. *SADABS*, 2008/2; Universität Göttingen, Göttingen, Germany, 2008.

(55) (a) Sheldrick, G. M. *Acta Crystallogr., Sect. A* **1990**, *46*, 467−473. (b) Sheldrick, G. M. *Acta Crystallogr., Sect. A* **2008**, *64*, 112−122. (c) Müller, P.; Herbst-Irmer, R.; Spek, A. L.; Schneider, T. R.; Sawaya, M. R. In *Crystal Structure Refinement—A Crystallographer's Guide to SHELXL, IUCr Texts on Crystallography*; Müller, P., Ed.; Oxford University Press: Oxford, U.K., 2006; Vol. *8*. (d) Hübschle, C. B.; Sheldrick, G. M.; Dittrich, B. *J. Appl. Crystallogr.* **2011**, *44*, 1281−1284.